The British Journal of Radiology, 79 (2006), 688–701

REVIEW ARTICLE

Non-invasive measurement of perfusion: a critical review of arterial spin labelling techniques

[1]E T PETERSEN, MSc, [1]I ZIMINE, PhD, [1]Y-C L HO, MSc and [1,2]X GOLAY, PhD

[1]*Department of Neuroradiology, National Neuroscience Institute and* [2]*Singapore Bioimaging Consortium, A*STAR, Singapore*

ABSTRACT. The non-invasive nature of arterial spin labelling (ASL) has opened a unique window into human brain function and perfusion physiology. High spatial and temporal resolution makes the technique very appealing not only for the diagnosis of vascular diseases, but also in basic neuroscience where the aim is to develop a more comprehensive picture of the physiological events accompanying neuronal activation. However, low signal-to-noise ratio and the complexity of flow quantification make ASL one of the more demanding disciplines within MRI. In this review, the theoretical background and main implementations of ASL are revisited. In particular, the perfusion quantification methods, including the problems and pitfalls involved, are thoroughly discussed in this article. Finally, a brief summary of applications is provided.

Received 15 December 2005
Accepted 29 March 2006

DOI: 10.1259/bjr/67705974

Perfusion, or the steady state nutritive delivery of blood to the tissue capillary bed, is vital for the homeostasis, and thereby survival, of an organ. Accurate perfusion measurement can provide important diagnostic information on pathological conditions, *e.g.* whether an ischaemic organ is viable or not. Among other methods, MRI has emerged as a powerful tool for assessing tissue perfusion and possesses strong diagnostic and prognostic capabilities, especially when combined with additional MRI modalities such as T_1, T_2 and diffusion-weighted images.

Historically, radiology has principally offered morphological imaging techniques; however, these new MRI perfusion techniques will add routine physiological imaging to its portfolio. This information is not only valuable in clinical settings, but is of great importance for basic physiological science and drug development, where, for example, perfusion changes due to a pharmacological stimulus might be monitored over time.

There exist two main MRI perfusion methods: bolus tracking after the injection of an exogenous endovascular tracer and arterial spin labelling (ASL), which uses magnetically labelled water protons as an endogenous tracer. The complete non-invasiveness of ASL makes it very suitable for perfusion studies of healthy volunteers and in patient groups requiring repetitive follow-ups. This is especially important in patients with particular conditions, such as kidney failure, or in paediatric populations where the use of radioactive tracers or exogenous contrast agents may be restricted. Recently, ASL has gained more clinical acceptance partly due to these advantages, but also as a result of the recently introduced technique for imaging the perfusion territory of individual blood vessels in the brain. In addition, the increased availability of high-field ($\geqslant$ 3 T) clinical scanners has moved ASL from the research and development stage towards the clinics.

The present article will focus on arterial spin labelling approaches. Different implementations and their advantages and disadvantages will be briefly reviewed. More attention will be given to the different ways of modelling the ASL data for perfusion quantification and the problems and pitfalls involved. Finally, research and clinical applications will be revisited.

Address correspondence to: Xavier Golay, Singapore Bioimaging Consortium, Agency for Science, Technology and Research (A*STAR), Singapore, 138667. E-mail: xavier_golay@sbic.a-star.edu.sg.

Methodology

Terminology

The term ''perfusion'' refers to the process involved in the nutritive blood delivery to the tissue's capillary bed. The physiology behind this blood delivery can be described by many different parameters, such as the blood flow itself, the volume of the blood vessels, the time it takes a particle, such as a red blood cell to traverse the vasculature. Finally, it can be described by the velocity of these particles. The results of 2D and 3D brain perfusion imaging techniques are commonly expressed as cerebral blood flow (CBF), which has a typical unit of [ml 100 ml^{-1} min^{-1}]. As noted, this is a rate [s^{-1}] rather than a volume-flux [m^3s^{-1}] measurement, which one would associate, for instance, with the flow from a pipe. This is, however, convenient, as the average flow rate is measured in a voxel of arbitrary volume. For historical reasons, CBF is often stated as [ml 100 $g^{-1}min^{-1}$], a

rather misleading unit because no information can be obtained about the tissue mass of the individual voxels and, in practice, a mean brain density of 1 g ml^{-1} is assigned to all voxels. The cerebral blood volume (CBV) describes the fraction of a voxel that contains blood vessels and is therefore dimensionless and usually expressed as [%] or [ml 100 g^{-1}]. Finally, the mean transit time (MTT) is the average time it takes a particle to traverse the vasculature [s]. These are the main parameters in general use, although measures such as time to peak concentration of the tracer (TTP) and flow heterogeneity (FH) can also be found in the perfusion imaging literature. All of them provide information about perfusion and are often referred to as perfusion maps.

Quantitative perfusion

In order to measure tissue perfusion, one needs to follow the course of blood flow through the organ, and for this there exist two methods, one based on freely diffusible and the other on intravascular tracers. As their names suggest, freely diffusible tracers can leave the intravascular space without restriction and be distributed throughout the entire tissue volume, whereas intravascular tracers remain in the vasculature, which constitutes only a fraction of the full volume.

Early perfusion experiments carried out by the pioneers Kety and Schmidt [1] used inhalation of free diffusible nitrous oxide (N_2O) as a tracer. This tracer distributes throughout the entire tissue volume, having a MTT in the order of minutes at normal physiological flow values. The relationship between the flow, distribution volume and the MTT is described by the central volume theorem, which states that the ratio between volume and flow is equal to the MTT. This rather long MTT allowed them to sample both arterial and venous blood, as arterial and venous tracer concentrations reached equilibrium after a few minutes. In this experiment, the time to reach this equilibrium is directly related to the cerebral blood flow using Fick's principle:

$$\frac{dC_t(t)}{dt} = \mathrm{CBF}(c_a(t) - c_v(t)) \quad (1)$$

where $C_t(t)$, $c_a(t)$ and $c_v(t)$ are the concentrations of tracer in the tissue, arterial and venous blood, respectively. The theory behind their method provides the basis for arterial spin labelling, which uses magnetically labelled water protons as the freely diffusible tracer.

However, when a freely diffusible tracer is used, there is no access to the blood volume and an intravascular tracer would be needed in order to obtain this volume information. In this case, the distribution volume is equal to the blood volume and using the terminology for the brain, then according to the central volume theorem: MTT = CBV/CBF. This principle is used in MRI bolus tracking experiments, where an intravascular tracer such as gadolinium-DTPA allows measurements of MTT, CBF and CBV. Here, the first pass of the bolus is monitored, an arterial input function (AIF) selected and based on the indicator-dilution theory of Meier and Zierler [2] and, a model-independent perfusion estimation can be obtained [3]. Time-domain impulse functions are employed to describe and compute the tissue perfusion CBF, which is calculated using the deconvolution of the tissue concentration curve $C_t(t)$ by the measured arterial input function $C_a(t)$:

$$C_t(t) = \mathrm{CBF} \cdot C_a(t) \otimes R(t) = \mathrm{CBF} \cdot \int_0^t C_a(\tau) R(t-\tau) d\tau \quad (2)$$

$R(t)$ is the residue function describing the fraction of contrast remaining in the system after a given time, t. If, alternatively, a steady state experiment is used, *i.e.* letting the contrast distribute to the total body blood volume, one can measure CBV by comparing images from before and after contrast. For recent reviews on these methodologies, see Østergaard et al, Grandin, Grenier et al, and Barbier et al [4–7].

The theory behind the two methods described above provides the basis for all applied perfusion measurement techniques used today. They range from MRI to CT and nuclear medicine imaging, all capable of measuring perfusion and/or blood volume in different parts of the body, depending on the selected tracer and imaging technique.

Perfusion imaging encompasses physiological mass transport and exchange mechanisms, where the system is required to be stationary, linear and time invariant in order to satisfy the underlying flow quantification theory. This means that no major physiological alterations are allowed during the acquisition scheme in order to obtain quantitative perfusion. This should be kept in mind when planning an experiment, especially when dealing with functional studies for instance, where the perfusion rate is manipulated over time.

Basic arterial spin labelling

The overall goal of all existing ASL techniques is to produce a flow-sensitized image or ''labelled'' image and a ''control'' image in which the static tissue signals are identical, but where the magnetization of the inflowing blood differs. The subtraction control-label yields a signal difference ΔM that directly reflects local perfusion because the signal from stationary tissue is completely eliminated (Figure 1). The label is usually performed by inverting or saturating the water molecules of the blood supplying the imaged region. By adding a delay between labelling and image acquisition, called inversion delay (TI), the labelled blood spins are allowed to reach the capillaries where they exchange with tissue water and thereby give rise to the perfusion signal. The signal difference, which is only 0.5–1.5% of the full signal, depends on many parameters such as the flow, T_1 of blood and tissue, as well as the time it takes blood to travel from the labelling to the imaging region. Multiple repetitions are needed for ensuring sufficient signal-to-noise, and a model of the perfusion signal is usually used in order to quantify the perfusion.

There exist two main classes of ASL techniques: continuous ASL (CASL) and pulsed ASL (PASL). In

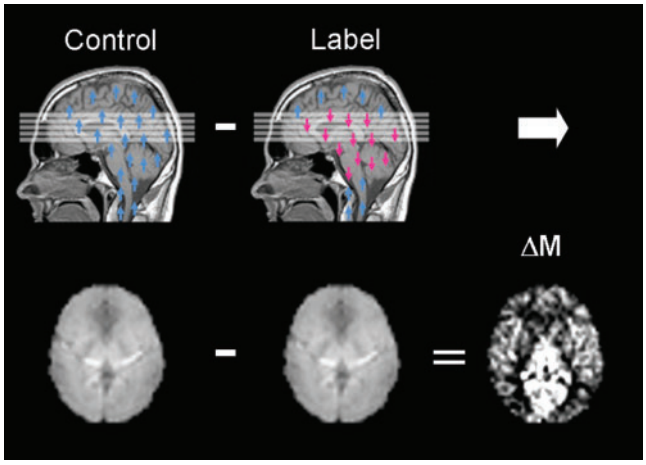

Figure 1. Schematic description of a perfusion weighted image (ΔM) obtained by subtraction of the labelled images from the control images.

CASL, the supplying blood is continuously labelled below the imaging slab, until the tissue magnetization reaches a steady state (Figure 2a). The PASL approach labels a thick slab of arterial blood at a single instance in time, and the imaging is performed after a time long enough for that spatially labelled blood to reach the tissue and exchange at the region of interest (Figure 2b). Both methods need a control experiment in order to visualize and quantify the perfusion.

Continuous arterial spin labelling

The original ASL method proposed by Williams et al [8, 9] in 1992 used a continuous flow-driven adiabatic inversion scheme, a method that was previously used for angiography [10]. This type of adiabatic inversion of the arterial magnetization is realized using a 2–4 s continuous radiofrequency (RF) pulse while applying a magnetic field gradient in the flow direction. The moving arterial spins will therefore experience a slow variation of the resonance frequency, which will result in their inversion, while static (tissue) spins will just be saturated. Typically, the inversion ''slice'' will be selected just proximal to the circle of Willis, near the medullospinal junction or at the level of the common carotid, and the spins in blood that flows through this plane will be inverted. The inversion efficiency α, which is important for further quantification, depends on factors like the mean velocity of the blood, angulations of the vessels to the plane and the selected RF amplitude and gradient strength. Typical labelling efficiency is in the range of 80–95% [8, 11–19].

Among the confounding factors of these long lasting inversion pulses are magnetization transfer (MT) effects [20]. When using a single coil for labelling and imaging, the off-resonance labelling pulse (with respect to imaging slice) will act as a powerful MT pulse in a way similar to an MT-weighted technique. The resulting saturation effect of the macromolecular pool will result in a reduced signal of the free water pool from the tissue of interest [21]. This is a very important issue, as the perfusion weighted images are calculated by subtracting

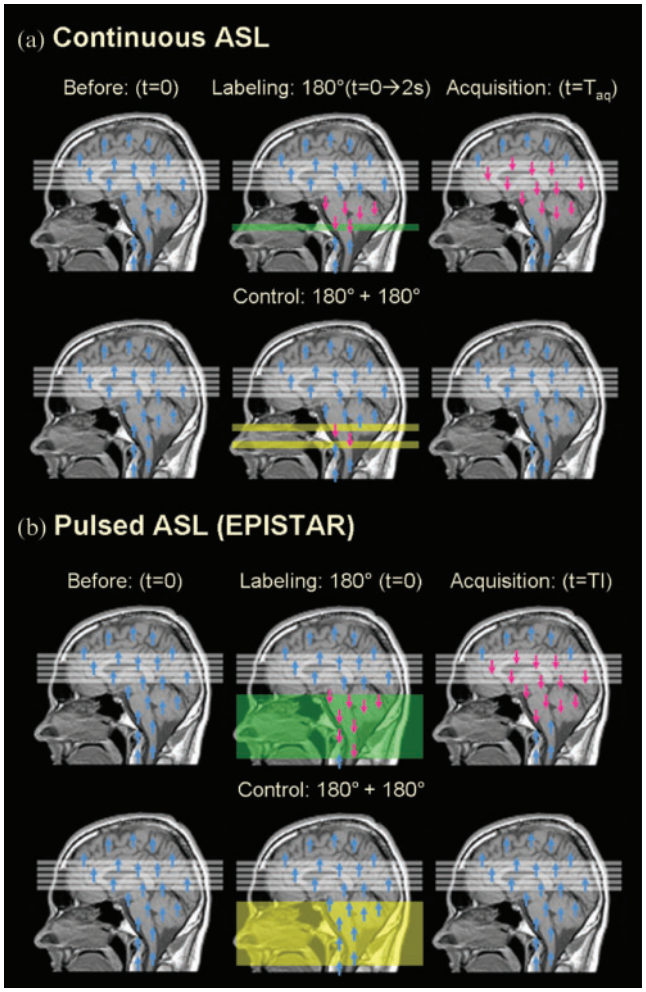

Figure 2. (a) Continuous arterial spin labelling (ASL) multislice experiment, using double adiabatic inversion for the control experiment, where labels get inverted during the passage of the first plane and returned to equilibrium during the subsequent passage of the second plane. (b) The EPISTAR pulsed ASL sequence, which labels everything at once and uses two $180^\circ + 180^\circ = 0^\circ$ pulses for the control images.

a labelled from a control acquisition, and if this MT effect is present only during the labelling scheme, it will lead to overestimated perfusion.

In the first implementation, these MT-effects were compensated for by applying a distal labelling during the control experiment. This produces identical saturation effects but, due to the applied gradients during labelling, this is unfortunately valid only for a single slice. For multislice acquisition, Alsop et al [22] proposed the use of two closely spaced inversion planes, also called double adiabatic inversion (DAI). In the control experiment, the magnetization gets inverted while traversing the first plane and returns theoretically to its original state during the passage through the second plane (the CASL experiment is shown in Figure 2a). Double inversion is achieved by applying a sinusoidal modulation of the RF waveform. Global control of the MT-effects is obtained by matching the RF power and the location of the planes. Figure 3 shows a perfusion map obtained using this method. Another method was also proposed, called simultaneously proximal and distal RF

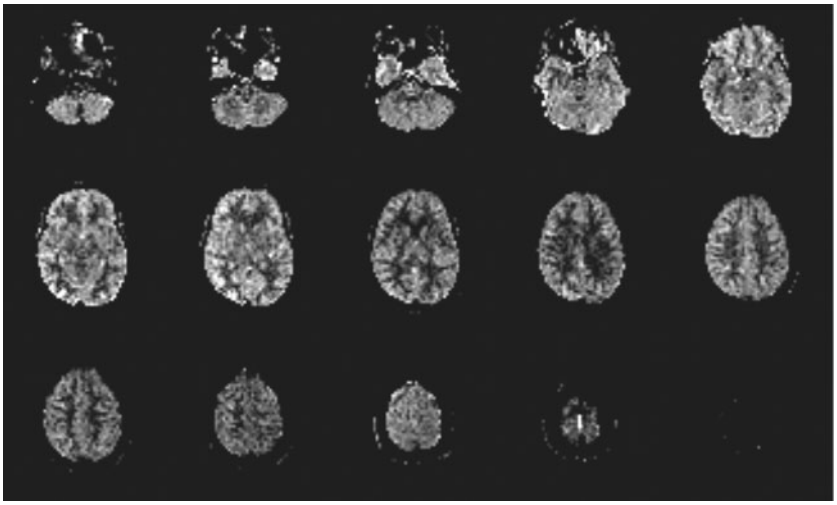

Figure 3. Full brain continuous arterial spin labelling (CASL) ΔM images acquired using double adiabatic inversion [22] in a healthy 27-year-old female. These images were acquired on a 1.5 T scanner of the F.M. Kirby Research Center for Functional Brain Imaging at Kennedy Krieger Institute.

irradiation (SPDI) for multislice acquisition [23]. In this later scheme, the RF power on the control scan is distributed evenly on both sides of the acquisition volume. However, a big limitation of these approaches is the doubled RF deposition, resulting in higher specific absorption rates (SAR). This is particularly important at higher field strength, and must be carefully considered for human studies at 3 Tesla and above.

Using two coils is another way of avoiding MT-effects and reducing the RF deposition [24–26]. In such methods, a small dedicated coil is used for labelling the carotid arteries and, due to the small physical extent of the applied RF field, no saturation occurs in the imaging region. Another advantage is that selective labelling of each carotid artery is possible, allowing independent mapping of the left- and right-internal carotid perfusion territories [27–29]. The main disadvantage of this approach is linked to the need for non-standard hardware, such as a separate transmit channel and a detuneable RF coil, which are not usually available on commercial clinical scanners. Another disadvantage of this approach is that the labelling takes place further away from the imaging slices, resulting in increased relaxation of the label before entering the imaging region. This approach has recently been applied for full brain coverage in humans at 3 Tesla without exceeding current SAR limits [30].

Pulsed arterial spin labelling

In 1994, Edelman et al [31] proposed the first pulsed ASL scheme. Contrary to CASL, the labelling is performed once in a 10–15 cm slab proximal to the image slices. For the PASL sequences, MT-effects have to be considered as well, although these are much smaller compared with CASL. In this first version of the ''Echo-Planar MR Imaging and Signal Targeting with Alternating Radio frequency'' (EPISTAR) sequence, inversion was performed distal to the image slice during the control experiment to induce identical MT effects in both cases. Again, this truly compensates for a single slice only and, therefore, the sequence was modified for multislice acquisition using a single 180° adiabatic pulse for the label experiment and two 180° + 180° pulses of half the power for the control experiment at the same proximal location (Figure 2b) [31, 32]. Figure 4 shows a multislice experiment using this technique.

Shortly afterwards, an alternative to this asymmetric method of labelling was proposed by Kwong et al [33] and independently by Kim [34], who named it flow alternating inversion recovery (FAIR). Here, the label is applied using a non-selective inversion pulse, while the control employs a concomitant slice selective gradient pulse. The symmetric nature of this sequence automatically compensates for MT-effects.

PASL allows inversion of the arterial spins closer to the image slices and the inversion efficiency α is improved; however, due to imperfect inversion profiles, a gap between the labelling region and the image slices of typically 1–2 cm is needed, depending on the type of RF pulse used. This increases transit time τ_a from the labelling slab to the imaging slices leading to decreased efficiency. In addition, T_1 relaxation of all the inverted spins will also result in a theoretically lower signal difference. Nevertheless, the ease of implementation and reduced practical problems, as compared with CASL, have made PASL a popular choice for perfusion imaging. This is reflected in the wide range of sequences available today, the common ones being listed in Table 1. For further in depth explanation of these sequences, see recent ASL reviews [4, 35].

ASL perfusion quantification

Having acquired the data using either technique, the subtracted control-label images will be perfusion weighted (Figure 1). The relationship between the ΔM signal and the actual CBF depends mainly on proton density and T_1 relaxation rates of tissue and inflowing blood, the and their respective differences. In addition, the label transit time from the inversion slab to the observed region in the images is also an important factor. Traditionally, quantitative CBF estimation is carried out using the tracer clearance theory originally proposed by Kety and Schmidt [1], which was first adapted to ASL experiments by Detre and Williams et al [8, 9]. In the

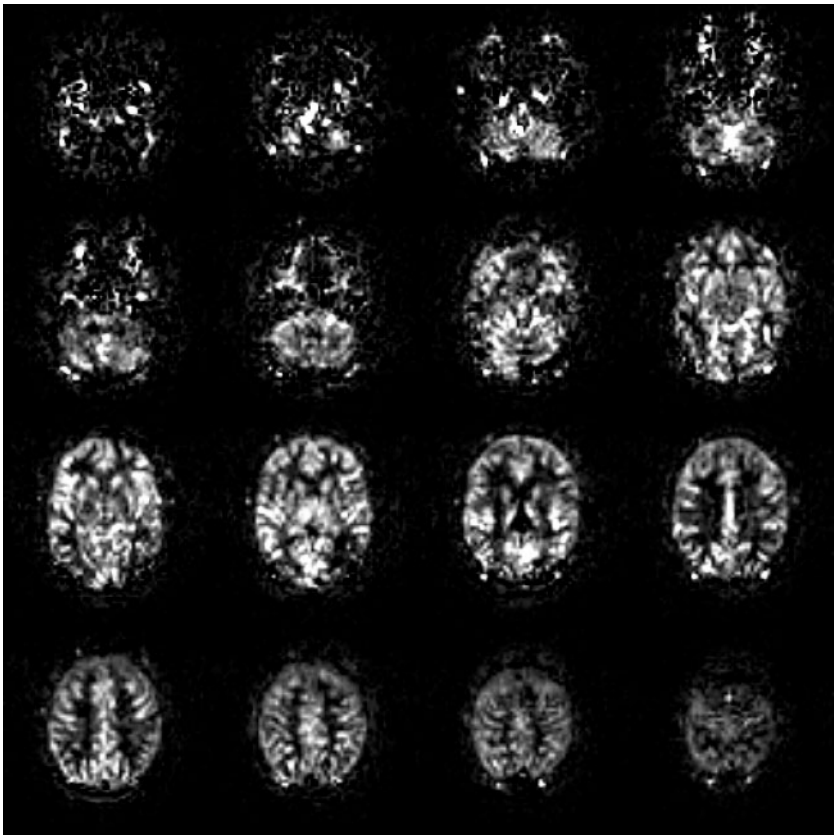

Figure 4. Full brain pulsed arterial spin labelling (PASL) using EPISTAR/PULSAR [32]. Images are the average of 30 control-label pairs acquired in 3 min using a T_R of 3 s and T_I of 1.7 s.

original model, it is assumed that the labelled arterial blood water is a free diffusible tracer, implying that the exchange of blood water with tissue water happens instantaneously upon its arrival to the parenchyma. Therefore, this model corresponds to a single compartment tracer kinetic, described by a mono-exponential tissue response function. The modified Bloch equation, including the flow dependent exchange term, becomes:

$$\frac{dM_t(t)}{dt} = \frac{M_{t,0} - M_t(t)}{T_{1t}} + \mathrm{CBF}\left(M_a(t) - \frac{M_t(t)}{\lambda}\right) \quad (3)$$

where M_t, $M_{t,0}$ and M_a are the tissue-, equilibrium- and arterial-magnetizations, respectively, λ is the blood–brain partition coefficient, and T_{1t} is the longitudinal relaxation rate of the tissue. In the original quantification model, further assumptions about uniform plug flow and equal T_1 relaxation of both tissue and arterial blood were made [8, 9].

Many derivatives and improved versions of this first solution exist for both CASL and PASL experiments. Calamante et al [36] took the difference in R_1 relaxation rate for tissue and arterial blood into account as well as

Table 1. Common arterial spin labelling sequences

Method	Sequence name	Reference
CASL (Asymmetric)	The original continuous arterial spin labelling	[8, 9, 120]
	DAI (Double Adiabatic Inversion)	[22]
(Symmetric)	SPDI (Simultaneously Proximal and Distal RF Irradiation)	[23]
(Two coil)	Two coil methods	[24, 25]
PASL (Asymmetric)	EPISTAR (Echo-Planar MR Imaging and Signal Targeting with Alternating Radio frequency)	[31]
	PICORE (Proximal Inversion with Control for Off-Resonance Effects)	[121]
	TILT (Transfer Insensitive Labelling Technique)	[44, 52]
	DIPLOMA (Double Inversion with Proximal Labelling of bOth tagged and control iMAges)	[122]
	STAR-HASTE (Signal Targeting with Alternating Radio frequency - HAlf-fourier Single shot Turbo spin-Echo)	[123]
	PULSAR (PULsed Star labelling of Arterial Regions)	[32]
	QUASAR (QUAntitative Star labelling of Arterial Regions)	[124]
(Symmetric)	FAIR (Flow Alternating Inversion Recovery)	[33, 34, 125]
	UNFAIR (UNinverted Flow Alternating Inversion Recovery)	[126]
	FAIRER (Flow Alternating Inversion Recovery Extra Radiofrequency pulse)	[127, 128]
	FAIRER (Flow Alternating Inversion Recovery Excluding Radiation damping)	[129, 130]
	BASE (unprepared BAsis and SElective inversion)	[52, 131]

CASL, continuous arterial spin labelling; PASL, pulsed arterial spin labelling.

the trailing edge τ_d of the bolus. In the work of Kwong et al [33], the transit time τ_a was also considered.

Buxton et al [37] proposed a general kinetic model where all the above mentioned parameters can be taken into account. Here, the magnetization difference between labelled and control measurements is described using the convolution integral in a way similar to Equation (2):

$$\Delta M = 2 \cdot M_{a,0} \cdot \mathrm{CBF} \cdot \int_0^t c(\tau) \cdot r(t-\tau) \cdot m(t-\tau) d\tau \qquad (4)$$

where $M_{0,a}$ is the equilibrium magnetization in a blood filled arterial voxel, $c(t)$ is the delivery function or fractional arterial input function (AIF). The residue function $r(t-\tau)$ describes the washout of labelled spins from a voxel, and $m(t-\tau)$ includes the longitudinal magnetization relaxation effects. The possibility to choose a particular arterial input function and to consider a certain exchange mechanism (single or multicompartment) allows greater flexibility for data analysis of both CASL and PASL experiments.

However, analytical solutions are only possible with simple assumptions, and the most widely used ''Standard Model'' can be summarized using the following terms:

$$c(t) = \begin{cases} 0, & t < \tau_a \\ \alpha \cdot e^{-t \cdot R_{1a}}, (\mathrm{PASL}) & \tau_a \le t < \tau_d \\ \alpha \cdot e^{-\tau_a \cdot R_{1a}}, (\mathrm{CASL}) & \tau_a \le t < \tau_d \\ 0, & t \ge \tau_d \end{cases} \qquad (5)$$

$$r(t) = e^{-\frac{CBF \cdot t}{\lambda}}$$

$$m(t) = e^{-t \cdot R_{1t}}$$

Again, the assumptions are: uniform plug flow and fast exchange, which is equivalent to single compartment kinetics. Solving Equation (5) using Equation (4) in the case of a PASL experiment gives a stepwise defined equation:

$$\Delta M(t) = \begin{cases} 0, & t < \tau_a \\ \frac{-2 \cdot a \cdot M_{a,0} \cdot CBF}{\delta R} e^{-R_{1a} \cdot t} \left(1 - e^{-\delta R \cdot (t-\tau_a)}\right), & \tau_a \le t < \tau_d \\ \frac{-2 \cdot a \cdot M_{a,0} \cdot CBF}{\delta R} e^{-R_{1a} \cdot \tau_d} \left(1 - e^{-\delta R \cdot (t-\tau_a)}\right) \cdot e^{-R_{1app} \cdot (t-\tau_d)}, & t \ge \tau_d \end{cases} \qquad (6)$$

where, $\delta R = R_{1a} - R_{1app}$ and $R_{1app} = R_{1t} + \mathrm{CBF}/\lambda$, also called the apparent tissue relaxation rate. A similar set of equations can be obtained for the CASL experiments, with the only difference being that $c(t)$ in Equation (5) is constant for CASL, whereas it is subject to T_{1a} decay for PASL, since the latter is not a steady-state method. As can be seen, various parameters like the transit time τ_a, blood–tissue partition coefficient λ, $M_{\alpha,0}$, R_{1a} and R_{1t} need to be estimated or measured in order to obtain quantitative CBF values. The difference between the many ASL sequences is mainly in the measurement (or not) of these parameters.

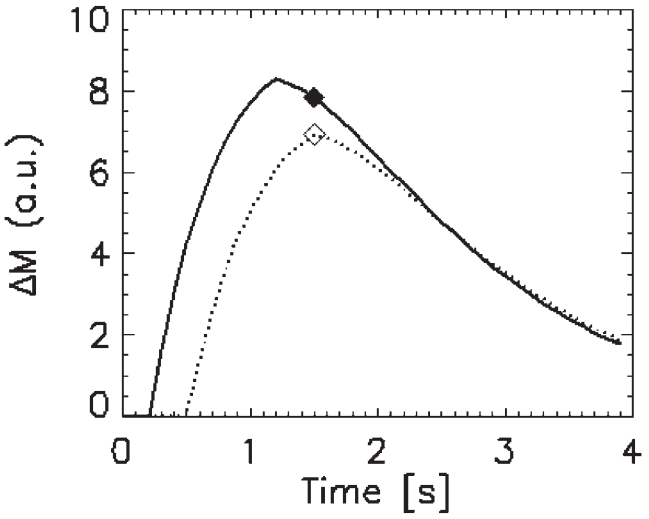

Figure 5. Diagram on an arterial spin labelling (ASL) time course. In this graph, an example of two voxels having the same flow (60 ml 100 g^{-1} min^{-1}) and relaxation characteristics, but different arrival time, is presented. The measured signal at a single inversion time of 1.5 s would result in a 12% lower ΔM signal in a voxel with delayed arrival of 500 ms (open square) as compared with a voxel with an arrival time of 200 ms (closed square).

Different issues relating to the actual perfusion quantification, using a single or multiple inversion time points, and the possible errors introduced using the standard model *vs* more advanced methods, will be discussed next.

Quantification errors

Transit time

The major source of error in the quantitative estimate of cerebral perfusion is the arterial transit time, τ_a, which even in healthy subjects differs across the brain, being longest in distal branches, especially in the regions between perfusion territories also known as border-zone areas. In most PASL approaches, information on perfusion is assessed at a single inversion time point (Figure 5), and therefore without information about the transit time. Quantification is then based on the second step in Equation (6), either where τ_a is assumed equal all over, or simply set to zero. The problem in doing this is that not only is the quantification of CBF impossible, but relative perfusion values between regions are not valid either. Sequences like QUIPSS II and Q2-TIPS [38, 39] were developed to render ASL more transit-time insensitive. Constant bolus duration is assured by saturating the part of the label that remains within the labelling slab at a time delay short enough to be able to intersect the trailing edge of the fastest blood. Appropriate timing of this saturation and the following image acquisition makes these sequences insensitive to the transit time. This is really an advantage in volunteers and patients without vascular diseases where the difference in transit time is small (<1.5 s) [40], as well as for quantitative functional studies where it is known

that the transit time changes are small (0.1–0.2 s) between baseline and activation conditions [41, 42].

However, these methods will fail in patients with atherosclerosis, where the transit time can be long in affected areas (>2.0 s) due to low perfusion velocity and, in some cases, extensive collateral perfusion. In these cases, the problem can be solved by acquiring images at multiple inversion times and therefore measuring the entire ΔM curve (Figure 6). The standard sequences, in which a single time point is acquired at a time (2–4 min per time point) are generally too lengthy to be suitable for clinical examinations [37, 41]. Günther et al [43] introduced an elegant solution to this problem using a Look-Locker-like readout to measure the ASL signal at multiple inversion times in a single scan (Figure 6). Because of multiple low flip angle readouts, the general model needs to be modified by substituting R_{1app} in Equation (6) with $R_{1app,eff} = R_{1t} + CBF/\lambda - \ln(\cos\phi)/\Delta TI$, where ϕ is the flip angle and ΔTI is the interval between the excitation pulses. A similar scheme was recently implemented using the transfer insensitive labelling technique (TILT) [44] by Hendrikse et al [45].

CASL is also sensitive to the transit time, but because of the steady state behaviour of this type of sequences, the effect is smaller than in PASL. Further improvements can be achieved using a pre-delay of typically 0.9–1.5 s between the continuous labelling and the readout, which renders CASL methods almost insensitive to transit time differences [46]. However, the duration of the delay should be chosen according to the subject's condition; in a healthy volunteer, a delay of 1 s would be suitable, while in patients with cerebrovascular diseases, longer delays are necessary [46].

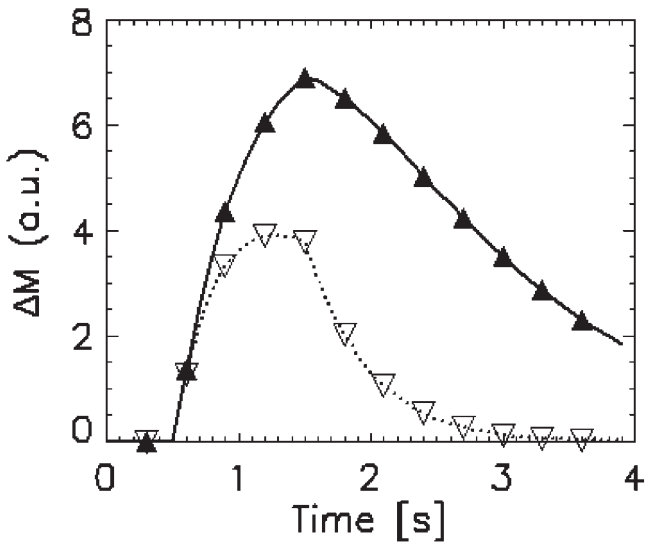

Figure 6. Dynamic perfusion characterization. In this time-course diagram, the black triangles show an example of repeated acquisition at multiple inversion time points. Usually, a three-parameter fit model is applied [37] to estimate cerebral blood flow (CBF) when multiple inversion times arterial spin labelling (ASL) sequences are used, which reveal additional information about arrival time and bolus duration. The second time-course (white triangles) has been calculated with identical perfusion parameters, while taking into account a Look-Locker readout method [43, 45, 124] (flip angle = 30°). The advantage of this method is a higher signal to noise ratio (SNR) as per acquisition time.

Vascular artefacts

Vascular artefacts, associated with the inflow of labelled arterial blood into the arteries, can introduce important errors in CBF quantification. Strictly speaking, for Equation (5) to be valid, none of the ΔM signal should originate from within the arterial vasculature. This assumption is often violated in voxels containing feeding vessels or traversing arteries, resulting in a substantial overestimation of perfusion values. Ye et al [47] proposed the use of bipolar crusher gradients to eliminate the signal from the large feeding arteries in CASL experiments. This was also adapted for PASL sequences. Another solution is to choose a sufficiently long inversion time, allowing the feeding vessels to empty before acquisition [40, 46–48].

Inversion pulse shape and efficiency

In PASL sequences, where a spatially defined label is used, the shape of the inversion pulse is of great importance. Ideally, the profile should be truly rectangular, allowing zero spacing between the labelling slab and the imaging region; due to finite duration of the RF pulse, this is not realizable in practice. Imperfect profile can reduce labelling efficiency, but, more importantly, there can be contamination in the imaging region from the labelling slab. To avoid this, a gap between the inversion and image plane is often introduced, with increased transit times as a result. In order to minimize this gap, longer adiabatic pulses like the hyperbolic secant (HS) [49], frequency offset corrected inversion (FOCI) [50] or bandwidth-modulated adiabatic selective saturation and inversion (BASSI) [51] pulses are often used. Another approach, as implemented in the TILT sequence [44], is the self-refocusing concatenated 90° Shinar-Leroux pulse combination that maintains the profile efficiency of the 90° pulses [52].

For CASL labelling, where labelling is performed in general at a distance from the imaging slices, the ''profile'' is less of a concern. It is the fulfilment of the adiabatic condition ensuring proper inversion that can be problematic [9, 15, 16, 22, 53].

Signal to noise issues

At normal perfusion rates of 40–100 ml 100 g^{-1} min^{-1} the signal change ΔM is in the order 0.5–1.5% of the full signal. Therefore, an average from typically 30 to 40 pairs of subtracted control and labelled images are required to get the desired signal to noise ratio (SNR) in the perfusion-weighted maps. A total scan time of 3–4 min is needed in order to acquire these data, which makes the technique very sensitive to motion artefacts. Proper head fixation and collaboration of the subject are necessary in order to obtain good results. Fast imaging techniques like single shot EPI and spiral sequences are often used to reduce the scan time between successive control-label

pairs as well as overall scan time. Also, prior saturation of the image plane reduces the sensitivity to motion. In case of limited motion, realignment of the images can improve quantification, but in general it is compromised because of low resolution, small number of slices, and small ΔM signal.

Finally, the running state of the scanner is important. Having a perfusion signal ΔM at only a fraction of the full signal, a slight drop in the scanner performance can preclude acquisition of clinically relevant ASL images, even if no effects can be detected in the standard clinical images.

Fast vs intermediate water exchange

The complex nature of the brain vasculature might not act like a single compartment to water based tracers. In particular, the blood–brain barrier seals the vasculature from the extravascular space, allowing a dynamic interface that protects the brain from toxic substances while allowing nutrients and other essential compounds to pass and thereby maintain its homeostasis. The ''free diffusible'' water is known to be limited to ''free'' diffusion through the lipid membrane of the endothelial cells as well as through dedicated water channels [54, 55], whereas diffusion in between adjacent endothelial cells is impossible due to tight junctional complexes [56].

The speed of the exchange in comparison with the 2–5 s duration of the ''control'' or ''label'' experiment still remains controversial. At higher flow rates, the exchange appears restricted [54], as though the water channels have been saturated. In order to deal with these effects, a few groups have suggested more elaborate multicompartmental approaches [57–59]. In general, the conclusion is that these effects are negligible at normal human perfusion rates at 1.5 Tesla, whereas the effect might be more pronounced when going toward higher field strengths. However, the intrinsic low SNR of the ASL techniques combined with the problems related to fitting all these additional exchange parameters will keep these models within the animal experimental world for at least another few years.

Bolus dispersion

Even when using vascular crushing and modelling assuming multicompartmental behaviour, it still leaves another possible error source, namely the dispersion of the labelled bolus. In a PASL experiment the label is close to being rectangular at the time of labelling and if the blood does not experience any resistance, this shape would persist all the way to the image slices. In reality, the blood friction with the vessel wall, resistance in bifurcations and the pulsatile behaviour of the flow make the flow profile look like something between a parabolic and ideal plug flow profile [60]. This results in dispersion of the bolus while it travels from the labelling slab to the imaging region, which will lead to underestimation of the perfusion.

Various attempts to incorporate these effects in the modelling have been made, and Hrabe et al [61] recently provided two analytical solutions that might reflect the physiology better. While the dispersion might be fairly homogeneous in healthy volunteers, patients with vascular diseases can be expected to have completely different dispersion in affected areas, and the flow estimation using these advanced models would still be non-quantitative.

Blood–brain partition coefficient

When a tracer consists of water or is dissolved in water, it is necessary to know the ratio of water in the tissue of interest and the feeding blood water in order to correct the distribution volume and thereby obtain the correct perfusion values. In the ASL technique, this is more related to the proton density, which tells us about how much signal we can expect from different tissues.

This ratio is called the blood–brain partition coefficient λ, and it was first defined by Kety [62] and corrected by Herscovitch et al [63] to the commonly used values today: whole brain $\lambda = 0.9$ ml g^{-1}, grey matter $\lambda_g = 0.98$ ml g^{-1} and white matter $\lambda_w = 0.82$ ml g^{-1}.

The relevance of this coefficient is controversial; first of all because the valid use of it requires instantaneous exchange of the tracer, which, as earlier mentioned, can be questionable, but also due to the fact that Roberts et al [64] demonstrated that this coefficient not only varies between different tissues, but also from region to region. Nevertheless, a whole brain value of 0.9 ml g^{-1} is commonly used for the calculations. Notice the unit of ml g^{-1}, which means that the unit of CBF/λ in Equation (5) becomes s^{-1} when CBF is expressed as ml g^{-1} s^{-1}.

Blood equilibrium magnetization

The inflowing blood has a proton density different from the tissue. For absolute quantification, the equilibrium magnetization of the arterial blood $M_{a,0}$ is needed, *i.e.* the available longitudinal magnetization from a fully relaxed blood filled voxel. This could be obtained from a partial volume-free arterial voxel, but with a standard in-plane resolution of 3–4 mm this is not possible in practice. Alternatively, this information can be taken from the much larger sagittal sinus. However, the T_2* of the deoxygenated venous blood, especially at higher field strength, is shorter than that of arterial blood. This results in a underestimated $M_{a,0}$. A different approach is to measure the equilibrium magnetization in a grey or white matter region and estimate $M_{a,0}$ using the blood–brain partition coefficient. For single inversion time experiments, this is often done on a voxel by voxel basis using the control experiment as $M_{t,0}$-map after correction for T_R and T_1.

Note that $M_{a,0}$ is a direct scaling factor of the perfusion (Equation (6)) and therefore an error in the product $\alpha \cdot M_{a,0}$ will directly change the calculated CBF value.

Functional studies and non-steady state perfusion

Finally, a requirement for using the various models and formulae for perfusion quantification is that tissue perfusion is a stationary, linear and time invariant

system. This would most often be satisfied in standard perfusion scans where the subject is resting. However, ASL has gained more and more popularity in functional studies where perfusion is monitored during various stimulation paradigms. Here, a typical experiment would have a repetition time of 2–3 s, while 4–6 s would be needed in order to acquire both control and label. Now, in functional experiments, the haemodynamic response time is often in the same range, which results in a violation of the steady state requirement [65, 66]. Not only will the flow change in between the control and label experiment, but also in between labelling and acquisition.

Two main problems arise from this; first, the models do not assume increasing or decreasing perfusion during the experiment and calculation errors will occur, and second, and probably the most important, is that T_2* will change due to the BOLD effect, which will reduce the signal intensity changes when acquiring at typical echo times of 15–25 ms.

In the case of a standard block paradigm, where the rising edges are discarded in the statistical analysis, this is not a problem. With basic research moving towards the characterization of the haemodynamic response on the other hand, the information in the rising and the falling edges are especially important. Recently, Lu et al [67] proposed a new subtraction method for reducing the T_2* effect, which is very suitable for this type of experiments, however, without addressing the problem of non-steady-state regimen.

Comparison with other imaging modalities

At this point, it should be kept in mind that related issues such as the ones highlighted in the previous paragraphs apply to other perfusion modalities like DSC-MRI, CT-perfusion and positron emission tomography (PET) as well. Dynamic susceptibility contrast using tracers such as gadolinium-DTPA for instance, suffers from the fact that the relationship between measured signal and contrast is non-linear and depends on parameters such as the field strength, shim of the magnet and the constitution of the vessels [68]. In addition, correct scaling of the AIF is influenced by partial volume effects in the voxels from where it is measured. Altogether, this makes quantification troublesome, and in the general clinical practice only a relative perfusion measure is possible. Similar problems exist in CT-perfusion, mainly related to the extraction of the global AIF [69]. PET can be said to be a more ''pure'' method for measuring perfusion due to the use of free diffusible tracers and experimental durations that ensure a steady state. However, a relatively low resolution of typically 6–10 mm introduces partial volume effects, *i.e.* a mixture of grey-matter, white-matter and CSF will be present in almost all voxels, making direct comparisons to the abovementioned methods questionable.

Applications

Despite the problems related to the quantification of perfusion using ASL, this technique has been used in numerous applications, ranging from basic neuroscience using animal models and human volunteers to clinical perfusion measurement in pathologies such as stroke and brain tumours. Furthermore, as long as the same procedure and parameters are consistently used, reproducible results can be achieved using ASL. Also the fact that most clinical decisions can be based on relative differences in perfusion rather than absolute measures could render this method useful in the daily clinical practice.

Although most publications on ASL to date have focused on brain perfusion, other organs like the lungs, kidneys and the heart have recently gained attention with improved techniques and hardware available. In particular, the move toward 3 T high field scanners in the standard clinical environments seems to push this method from the research and development stage towards clinical applications.

The various applications of ASL have recently been extensively covered elsewhere [4, 35] and only a short summary of the active fields and most recent applications will be listed here. Two main categories exist – the basic science, mainly neuroscience, and the general clinical use.

Neuroscience

The ability to measure CBF is very important for the assessment of tissue metabolism and function. The complete non-invasiveness of ASL, which allows prolonged functional studies to be performed on any volunteer, makes it a preferable choice in many neuroscience applications. Following a neuronal activation paradigm, the classical blood oxygen level dependent (BOLD) contrast [70] is a result of T_2* changes due to alterations of CBF and CBV, as well as the cerebral metabolic rate of oxygen uptake ($CMRO_2$). The ASL signal, on the other hand, is an absolute measure of CBF changes, which makes this technique more reproducible over time, as well as in between subjects [71–73]. In addition, perfusion functional MRI (fMRI) is believed to localize regions of activation more accurately [74], contrary to BOLD, which is affected by the change in deoxygenated blood in draining venous vessels resulting in additional signal from ''down stream'' areas. In addition to flow information, the BOLD signal can also be extracted from an ASL [75, 76]. Recent research using these techniques includes: Lu et al [77], who combined ASL, BOLD and vascular space occupancy (VASO) and Obata et al [78], who applied the ''balloon model'' to simultaneously acquire BOLD and ASL data. Finally, Hoge et al [79] combined optical and ASL imaging methods. All three studies were aimed at developing a more comprehensive picture of the physiological events accompanying activation.

For pharmaceutical validation, the suitability of ASL for prolonged functional studies is advantageous for studying perfusion-altering drugs. Alternative techniques often require the injection of a tracer, which cannot be repeated more than a few times and would possibly interfere with the drug itself. Among investigated pharmaceutical agents are the vasodilators acetazolamide [80, 81] and 2-chloradonosine [82, 83], as well as

the vasoconstrictor indomethacin [84, 85] and finally isoflurane, which is used for anaesthesia [86, 87]. This field can be expected to expand with broader awareness of ASL and availability of the sequences used.

Clinical

In the clinics, an important issue is how well ASL performs when compared with established ''gold-standard'' methods. Validation studies have been carried out in animals [57, 88, 89] using radioactive microspheres and ^{14}C-iodoantipyrine autoradiography, as well as in humans [90] comparing ASL and PET. In general, good correlation is observed for grey matter, whereas white-matter often shows an underestimation of CBF. This is mainly attributed the prolonged arrival times and low perfusion values of white matter, which is in the lower range of measurable flow values using ASL.

The benefits of ASL particularly suit the requirements of the paediatric population, where there is a need to avoid ionizing radiation as procedures are likely to be repeated for disease monitoring and venous cannulation can be highly traumatic. In addition, the general higher blood flow seen in children increases the difference signal ΔM and thereby the perfusion SNR [91], making ASL a very promising tool for paediatric perfusion studies [92].

Another particularly appropriate clinical arena is that of cerebrovascular diseases. In fact, stroke is the third cause of death behind cardiovascular diseases and cancer. Consequently, a lot of resources are put into the research of this disease – how to prevent it, the immediate therapy following stroke and post-stroke rehabilitation procedures. In recent years, ASL techniques have become an alternative tool to CT and bolus tracking MRI for studying the mechanisms of stroke and the underlying processes of brain damage resulting from ischaemia. Studies of the evolution of acute stroke and validation of outcome predictors for the identification of potentially salvageable tissue have been performed in animal models [93–96] and patients [97, 98] using both PASL and CASL. For the assessment of the different perfusion territories and eventually collateralized flow in steno-occlusive patients, a range of ASL sequences has been made capable of labelling individual perfusion territories of the major feeding vessels one at a time [24, 27, 28, 32, 99–102]. An example of regional perfusion imaging of a healthy volunteer is shown in Figure 7. These techniques are very promising in the evaluation of the successful recruitment of subsidiary blood vessels, which are believed to play an important role in the clinical outcome of patients with cerebral artery occlusion. Until recently, diagnostic strategies to evaluate the collateral circulation could be divided into those that directly visualized collateral blood vessels, such as conventional X–ray angiography and indirect methods that assess tissue perfusion, including acetazolamide-challenge tests of cerebrovascular reserve. This new class of ASL techniques makes the combination of both methods possible for the first time and quantitative information of the flow territories supplied by each major brain vessel is obtainable. As such, these methods could become alternatives to conventional X–ray based subtraction angiography, which is so far the only modality giving temporal as well as spatial regional blood flow information. Using these techniques, Van Laar et al [103] showed a wide interindividual variability in the perfusion territories caused mainly by anatomical variations of the circle of Willis in a population study of 115 healthy ageing volunteers.

ASL has also been used in the evaluation of cancer. The perfusion change in tumours depends on their aggressiveness or grade, which makes perfusion information important when selecting and evaluating therapies. Repeated ASL perfusion measurements can be used to monitor the effect of blood flow regulating agents and other anticancer therapeutics such as anti–angiogenic agents [104–107].

Finally, ASL has also been applied to organs other than the brain, although the majority of research and applications have focused on the latter. Applications range from

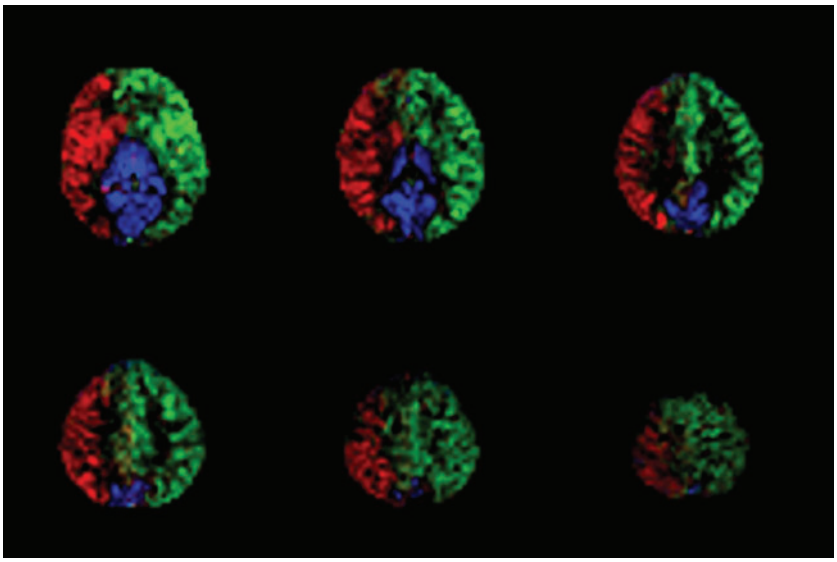

Figure 7. Regional perfusion image (RPI) acquired using QUASAR [124] on a 23-year-old healthy female subject.

combined lung perfusion using ASL and ventilation scans using hyperpolarized helium-3 for evaluation of pulmonary diseases [108–111], to cardiac [112–114] and renal [6, 115–119] perfusion imaging. However, these techniques are very challenging, mainly due to non-rigidity and increased movement of these organs as compared with the brain.

Conclusion

The evolution of ASL since its invention by Williams et al [8, 9] in 1992 is remarkable. Numerous sequences have been developed, each solving problematic issues such as magnetization transfer effects, insensitivity to transit times etc. in their own way. Along the way, the quantitative aspect has been the leading factor and various models have been proposed for absolute CBF quantification. However, there are still improvements to be made and, with the move from traditional brain perfusion imaging to abdominal organs, there are certainly more challenges ahead.

Despite the remarkable progress, ASL has still not overtaken traditional invasive methods in the clinics. One reason for this is the intrinsically low SNR, making averaging necessary, and therefore good cooperation from the subject is essential. This is not always the case with, for instance, stroke patients or children. Nevertheless, the great improvements in hardware and the increasing availability of high field clinical scanners pre-installed with ASL sequences seem to put more focus on these techniques. Robust sequences for regional perfusion imaging and functional studies of either cognitive or pharmacological nature are also gaining more and more interest, and the complete non-invasiveness of these techniques will always be an attractive asset.

Acknowledgments

The authors would like to thank Prof. Alan Jackson for the opportunity to write this review article. This work was supported in part by Philips Medical Systems, and the following grants: # NMRC/0855/2004, NMRC/CPG/009/2004, NMRC/0919/2004 and NHGA-RPR/04012.

References

1. Kety SS, Schmidt CF. The nitrous oxide method for the quantitative determination of cerebral blood flow in man: theory, procedure and normal values. J Clin Invest 1948;4:476–83.
2. Meier P, Zierler KL. On the theory of the indicator-dilution method for measurement of blood flow and volume. J Appl Physiol 1954;6:731–44.
3. Ostergaard L, Weisskoff RM, Chesler DA, Gyldensted C, Rosen BR. High resolution measurement of cerebral blood flow using intravascular tracer bolus passages. Part I: Mathematical approach and statistical analysis. Magn Reson Med 1996;36:715–25.
4. Barbier EL, Lamalle L, Decorps M. Methodology of brain perfusion imaging. J Magn Reson Imaging 2001;13:496–520.
5. Grandin CB. Assessment of brain perfusion with MRI: methodology and application to acute stroke. Neuroradiology 2003;45:755–66.
6. Grenier N, Basseau F, Ries M, Tyndal B, Jones R, Moonen C. Functional MRI of the kidney. Abdom Imaging 2003;28:164–75.
7. Ostergaard L. Cerebral perfusion imaging by bolus tracking. Top Magn Reson Imaging 2004;15:3–9.
8. Williams DS, Detre JA, Leigh JS, Koretsky AP. Magnetic resonance imaging of perfusion using spin inversion of arterial water. Proc Natl Acad Sci USA 1992;89:212–6.
9. Detre JA, Leigh JS, Williams DS, Koretsky AP. Perfusion imaging. Magn Reson Med 1992;23:37–45.
10. Dixon WT, Du LN, Faul DD, Gado M, Rossnick S. Projection angiograms of blood labeled by adiabatic fast passage. Magn Reson Med 1986;3:454–62.
11. Zhang W, Williams DS, Koretsky AP. Measurement of rat brain perfusion by NMR using spin labeling of arterial water: in vivo determination of the degree of spin labeling. Magn Reson Med 1993;29:416–21.
12. Maccotta L, Detre JA, Alsop DC. The efficiency of adiabatic inversion for perfusion imaging by arterial spin labeling. NMR Biomed 1997;10:216–21.
13. Utting JF, Thomas DL, Gadian DG, Ordidge RJ. Velocity-driven adiabatic fast passage for arterial spin labeling: results from a computer model. Magn Reson Med 2003;49:398–401.
14. Franke C, van Dorsten FA, Olah L, Schwindt W, Hoehn M. Arterial spin tagging perfusion imaging of rat brain: dependency on magnetic field strength. Magn Reson Imaging 2000;18:1109–13.
15. Gach HM, Dai W. Simple model of double adiabatic inversion (DAI) efficiency. Magn Reson Med 2004;52:941–6.
16. Gach HM, Kam AW, Reid ED, Talagala SL. Quantitative analysis of adiabatic fast passage for steady laminar and turbulent flows. Magn Reson Med 2002;47:709–19.
17. Trampel R, Jochimsen TH, Mildner T, Norris DG, Moller HE. Efficiency of flow-driven adiabatic spin inversion under realistic experimental conditions: a computer simulation. Magn Reson Med 2004;51:1187–93.
18. Werner R, Norris DG, Alfke K, Mehdorn HM, Jansen O. Improving the amplitude-modulated control experiment for multislice continuous arterial spin labeling. Magn Reson Med 2005;53:1096–102.
19. Marro KI, Hayes CE, Kushmerick MJ. A model of the inversion process in an arterial inversion experiment. NMR Biomed 1997;10:324–32.
20. Wolff SD, Balaban RS. Magnetization transfer contrast (MTC) and tissue water proton relaxation in vivo. Magn Reson Med 1989;10:135–44.
21. Henkelman RM, Huang X, Xiang QS, Stanisz GJ, Swanson SD, Bronskill MJ. Quantitative interpretation of magnetization transfer. Magn Reson Med 1993;29:759–66.
22. Alsop DC, Detre JA. Multisection cerebral blood flow MR imaging with continuous arterial spin labeling. Radiology 1998;208:410–6.
23. Talagala SL, Barbier EL, Williams DS, Silva AC, Koretsky AP. Multi-slice perfusion MRI using continuous arterial water labeling controlling for MT effects with simultaneous proximal and distal RF irradiation. Proceedings of the 6th Annual Meeting of ISMRM, Sydney, 1998.
24. Zhang W, Silva AC, Williams DS, Koretsky AP. NMR measurement of perfusion using arterial spin labeling without saturation of macromolecular spins. Magn Reson Med 1995;33:370–6.
25. Silva AC, Zhang W, Williams DS, Koretsky AP. Multi-slice MRI of rat brain perfusion during amphetamine stimulation using arterial spin labeling. Magn Reson Med 1995;33:209–14.
26. McLaughlin AC, Ye FQ, Pekar JJ, Santha AK, Frank JA. Effect of magnetization transfer on the measurement of cerebral blood flow using steady-state arterial spin tagging

approaches: a theoretical investigation. Magn Reson Med 1997;37:501–10.
27. Zaharchuk G, Ledden PJ, Kwong KK, Reese TG, Rosen BR, Wald LL. Multislice perfusion and perfusion territory imaging in humans with separate label and image coils. Magn Reson Med 1999;41:1093–8.
28. Mildner T, Trampel R, Moller HE, Schafer A, Wiggins CJ, Norris DG. Functional perfusion imaging using continuous arterial spin labeling with separate labeling and imaging coils at 3 T. Magn Reson Med 2003;49:791–5.
29. Floyd TF, Ratcliffe SJ, Wang J, Resch B, Detre JA. Precision of the CASL-perfusion MRI technique for the measurement of cerebral blood flow in whole brain and vascular territories. J Magn Reson Imaging 2003;18:649–55.
30. Talagala SL, Ye FQ, Ledden PJ, Chesnick S. Whole-brain 3D perfusion MRI at 3.0 T using CASL with a separate labeling coil. Magn Reson Med 2004;52:131–40.
31. Edelman RR, Siewert B, Darby DG, Thangaraj V, Nobre AC, Mesulam MM, et al. Qualitative mapping of cerebral blood flow and functional localization with echo-planar MR imaging and signal targeting with alternating radio frequency. Radiology 1994;192:513–20.
32. Golay X, Petersen ET, Hui F. Pulsed star labeling of arterial regions (PULSAR): a robust regional perfusion technique for high field imaging. Magn Reson Med 2005;53:15–21.
33. Kwong KK, Chesler DA, Weisskoff RM, Donahue KM, Davis TL, Ostergaard L, et al. MR perfusion studies with T1-weighted echo planar imaging. Magn Reson Med 1995;34:878–87.
34. Kim SG. Quantification of relative cerebral blood flow change by flow-sensitive alternating inversion recovery (FAIR) technique: application to functional mapping. Magn Reson Med 1995;34:293–301.
35. Golay X, Hendrikse J, Lim TC. Perfusion imaging using arterial spin labeling. Top Magn Reson Imaging 2004;15:10–27.
36. Calamante F, Kwong KK, Williams DS, van der GJ, Tyndal B. Quantification of perfusion in pulsed labeling techniques. Proceedings of the 3rd Annual Meeting of ISMRM, Nice, France, 870. 1995.
37. Buxton RB, Frank LR, Wong EC, Siewert B, Warach S, Edelman RR. A general kinetic model for quantitative perfusion imaging with arterial spin labeling. Magn Reson Med 1998;40:383–96.
38. Luh WM, Wong EC, Bandettini PA, Hyde JS. QUIPSS II with thin-slice TI1 periodic saturation: a method for improving accuracy of quantitative perfusion imaging using pulsed arterial spin labeling. Magn Reson Med 1999;41:1246–54.
39. Wong EC, Buxton RB, Frank LR. Quantitative imaging of perfusion using a single subtraction (QUIPSS and QUIPSS II). Magn Reson Med 1998;39:702–8.
40. Wang J, Alsop DC, Song HK, Maldjian JA, Tang K, Salvucci AE, et al. Arterial transit time imaging with flow encoding arterial spin tagging (FEAST). Magn Reson Med 2003;50:599–607.
41. Yang Y, Engelien W, Xu S, Gu H, Silbersweig DA, Stern E. Transit time, trailing time, and cerebral blood flow during brain activation: measurement using multislice, pulsed spin-labeling perfusion imaging. Magn Reson Med 2000;44:680–5.
42. Gonzalez-At JB, Alsop DC, Detre JA. Cerebral perfusion and arterial transit time changes during task activation determined with continuous arterial spin labeling. Magn Reson Med 2000;43:739–46.
43. Gunther M, Bock M, Schad LR. Arterial spin labeling in combination with a look-locker sampling strategy: inflow turbo-sampling EPI-FAIR (ITS-FAIR). Magn Reson Med 2001;46:974–84.
44. Golay X, Stuber M, Pruessmann KP, Meier D, Boesiger P. Transfer insensitive labeling technique (TILT): application to multislice functional perfusion imaging. J Magn Reson Imaging 1999;9:454–61.
45. Hendrikse J, Lu H, van der Grond J, van Zijl PC, Golay X. Measurements of cerebral perfusion and arterial hemodynamics during visual stimulation using TURBO-TILT. Magn Reson Med 2003;50:429–33.
46. Detre JA, Alsop DC, Vives LR, Maccotta L, Teener JW, Raps EC. Noninvasive MRI evaluation of cerebral blood flow in cerebrovascular disease. Neurology 1998;50:633–41.
47. Ye FQ, Mattay VS, Jezzard P, Frank JA, Weinberger DR, McLaughlin AC. Correction for vascular artifacts in cerebral blood flow values measured by using arterial spin tagging techniques. Magn Reson Med 1997;37:226–35.
48. Yang Y, Frank JA, Hou L, Ye FQ, McLaughlin AC, Duyn JH. Multislice imaging of quantitative cerebral perfusion with pulsed arterial spin labeling. Magn Reson Med 1998;39:825–32.
49. Silver MS, Joseph RI, Hoult DI. Selective spin inversion in nuclear magnetic resonance and coherent optics through an exact solution of the Bloch-Riccati equation. Physical Review A 1985;31:2753–5.
50. Ordidge RJ, Wylezinska M, Hugg JW, Butterworth E, Franconi F. Frequency offset corrected inversion (FOCI) pulses for use in localized spectroscopy. Magn Reson Med 1996;36:562–6.
51. Warnking JM, Pike GB. Bandwidth-modulated adiabatic RF pulses for uniform selective saturation and inversion. Magn Reson Med 2004;52:1190–9.
52. Pruessmann KP, Golay X, Stuber M, Scheidegger MB, Boesiger P. RF pulse concatenation for spatially selective inversion. J Magn Reson 2000;146:58–65.
53. Zhan W, Gu H, Silbersweig DA, Stern E, Yang Y. Inversion profiles of adiabatic inversion pulses for flowing spins: the effects on labeling efficiency and labeling accuracy in perfusion imaging with pulsed arterial spin-labeling. Magn Reson Imaging 2002;20:487–94.
54. Paulson OB, Hertz MM, Bolwig TG, Lassen NA. Water filtration and diffusion across the blood brain barrier in man. Acta Neurol Scand Suppl 1977;64:492–3.
55. Amiry-Moghaddam M, Frydenlund DS, Ottersen OP. Anchoring of aquaporin-4 in brain: molecular mechanisms and implications for the physiology and pathophysiology of water transport. Neuroscience 2004;129:999–1010.
56. Farquhar MG, Palade GE. Junctional complexes in various epithelia. J Cell Biol 1963;17:375–412.
57. Zhou J, Wilson DA, Ulatowski JA, Traystman RJ, van Zijl PC. Two-compartment exchange model for perfusion quantification using arterial spin tagging. J Cereb Blood Flow Metab 2001;21:440–55.
58. St Lawrence KS, Frank JA, McLaughlin AC. Effect of restricted water exchange on cerebral blood flow values calculated with arterial spin tagging: a theoretical investigation. Magn Reson Med 2000;44:440–9.
59. Li KL, Zhu X, Hylton N, Jahng GH, Weiner MW, Schuff N. Four-phase single-capillary stepwise model for kinetics in arterial spin labeling MRI. Magn Reson Med 2005;53:511–8.
60. Fung YC. Biomechanics: Circulation. 2nd edition, Springer-Verlag, New York. 11-21-1996.
61. Hrabe J, Lewis DP. Two analytical solutions for a model of pulsed arterial spin labeling with randomized blood arrival times. J Magn Reson 2004;167:49–55.
62. Kety SS. The theory and applications of the exchange of inert gas at the lungs and tissues. Pharmacol Rev 1951;3:1–41.
63. Herscovitch P, Raichle ME. What is the correct value for the brain--blood partition coefficient for water? J Cereb Blood Flow Metab 1985;5:65–9.

64. Roberts DA, Rizi R, Lenkinski RE, Leigh JS Jr. Magnetic resonance imaging of the brain: blood partition coefficient for water: application to spin-tagging measurement of perfusion. J Magn Reson Imaging 1996;6:363–6.
65. Friston KJ, Mechelli A, Turner R, Price CJ. Nonlinear responses in fMRI: the Balloon model, Volterra kernels, and other hemodynamics. Neuroimage 2000;12:466–77.
66. Friston KJ. Models of brain function in neuroimaging. Ann Rev Psychol 2005;56:57–87.
67. Lu H, Golay X, Pekar JJ, van Zijl PC. Noise or artifact: detrimental effects of BOLD signal in arterial spin labeling fMRI at high field strength. Proceedings of the 13th Annual Meeting ISMRM, Miami Beach, USA, #35. 2005.
68. Boxerman JL, Hamberg LM, Rosen BR, Weisskoff RM. MR contrast due to intravascular magnetic susceptibility perturbations. Magn Reson Med 1995;34:555–66.
69. Wintermark M, Sesay M, Barbier E, Borbely K, Dillon WP, Eastwood JD, et al. Comparative overview of brain perfusion imaging techniques. Stroke 2005;36:2032–3.
70. Ogawa S, Lee TM, Kay AR, Tank DW. Brain magnetic resonance imaging with contrast dependent on blood oxygenation. Proc Natl Acad Sci USA 1990;87:9868–72.
71. Aguirre GK, Detre JA, Zarahn E, Alsop DC. Experimental design and the relative sensitivity of BOLD and perfusion fMRI. Neuroimage 2002;15:488–500.
72. Detre JA, Wang J. Technical aspects and utility of fMRI using BOLD and ASL. Clin Neurophysiol 2002;113:621–34.
73. Wang J, Aguirre GK, Kimberg DY, Roc AC, Li L, Detre JA. Arterial spin labeling perfusion fMRI with very low task frequency. Magn Reson Med 2003;49:796–802.
74. Duong TQ, Kim DS, Ugurbil K, Kim SG. Localized cerebral blood flow response at submillimeter columnar resolution. Proc Natl Acad Sci USA 2001;98:10904–9.
75. Kim SG, Tsekos NV, Ashe J. Multi-slice perfusion-based functional MRI using the FAIR technique: comparison of CBF and BOLD effects. NMR Biomed 1997;10:191–6.
76. Kim SG, Ugurbil K. Comparison of blood oxygenation and cerebral blood flow effects in fMRI: estimation of relative oxygen consumption change. Magn Reson Med 1997;38:59–65.
77. Lu H, Golay X, Pekar JJ, van Zijl PC. Sustained poststimulus elevation in cerebral oxygen utilization after vascular recovery. J Cereb Blood Flow Metab 2004;24:764–70.
78. Obata T, Liu TT, Miller KL, Luh WM, Wong EC, Frank LR, et al. Discrepancies between BOLD and flow dynamics in primary and supplementary motor areas: application of the balloon model to the interpretation of BOLD transients. Neuroimage 2004;21:144–53.
79. Hoge RD, Franceschini MA, Covolan RJ, Huppert T, Mandeville JB, Boas DA. Simultaneous recording of task-induced changes in blood oxygenation, volume, and flow using diffuse optical imaging and arterial spin-labeling MRI. Neuroimage 2005;25:701–7.
80. Detre JA, Samuels OB, Alsop DC, Gonzalez-At JB, Kasner SE, Raps EC. Noninvasive magnetic resonance imaging evaluation of cerebral blood flow with acetazolamide challenge in patients with cerebrovascular stenosis. J Magn Reson Imaging 1999;10:870–5.
81. Yen YF, Field AS, Martin EM, Ari N, Burdette JH, Moody DM, et al. Test-retest reproducibility of quantitative CBF measurements using FAIR perfusion MRI and acetazolamide challenge. Magn Reson Med 2002;47:921–8.
82. Kochanek PM, Hendrich KS, Robertson CL, Williams DS, Melick JA, Ho C, et al. Assessment of the effect of 2-chloroadenosine in normal rat brain using spin-labeled MRI measurement of perfusion. Magn Reson Med 2001;45: 924–9.
83. Robertson CL, Hendrich KS, Kochanek PM, Jackson EK, Melick JA, Graham SH, et al. Assessment of 2-chloroadenosine treatment after experimental traumatic brain injury in the rat using arterial spin-labeled MRI: a preliminary report. Acta Neurochir Suppl 2000;76:187–9.
84. St Lawrence KS, Ye FQ, Lewis BK, Weinberger DR, Frank JA, McLaughlin AC. Effects of indomethacin on cerebral blood flow at rest and during hypercapnia: an arterial spin tagging study in humans. J Magn Reson Imaging 2002;15:628–35.
85. St Lawrence KS, Ye FQ, Lewis BK, Frank JA, McLaughlin AC. Measuring the effects of indomethacin on changes in cerebral oxidative metabolism and cerebral blood flow during sensorimotor activation. Magn Reson Med 2003;50:99–106.
86. Liu ZM, Schmidt KF, Sicard KM, Duong TQ. Imaging oxygen consumption in forepaw somatosensory stimulation in rats under isoflurane anesthesia. Magn Reson Med 2004;52:277–85.
87. Sicard K, Shen Q, Brevard ME, Sullivan R, Ferris CF, King JA, et al. Regional cerebral blood flow and BOLD responses in conscious and anesthetized rats under basal and hypercapnic conditions: implications for functional MRI studies. J Cereb Blood Flow Metab 2003;23:472–81.
88. Walsh EG, Minematsu K, Leppo J, Moore SC. Radioactive microsphere validation of a volume localized continuous saturation perfusion measurement. Magn Reson Med 1994;31:147–53.
89. Ewing JR, Wei L, Knight RA, Pawa S, Nagaraja TN, Brusca T, et al. Direct comparison of local cerebral blood flow rates measured by MRI arterial spin-tagging and quantitative autoradiography in a rat model of experimental cerebral ischemia. J Cereb Blood Flow Metab 2003;23: 198–209.
90. Ye FQ, Berman KF, Ellmore T, Esposito G, van Horn JD, Yang Y, et al. H(2)(15)O PET validation of steady-state arterial spin tagging cerebral blood flow measurements in humans. Magn Reson Med 2000;44:450–6.
91. Wang J, Licht DJ, Jahng GH, Liu CS, Rubin JT, Haselgrove J, et al. Pediatric perfusion imaging using pulsed arterial spin labeling. J Magn Reson Imaging 2003;18:404–13.
92. Oguz KK, Golay X, Pizzini FB, Freer CA, Winrow N, Ichord R, et al. Sickle cell disease: continuous arterial spin-labeling perfusion MR imaging in children. Radiology 2003;227:567–74.
93. Calamante F, Lythgoe MF, Pell GS, Thomas DL, King MD, Busza AL, et al. Early changes in water diffusion, perfusion, T1, and T2 during focal cerebral ischemia in the rat studied at 8.5 T. Magn Reson Med 1999;41:479–85.
94. Lythgoe MF, Thomas DL, Calamante F, Pell GS, King MD, Busza AL, et al. Acute changes in MRI diffusion, perfusion, T(1), and T(2) in a rat model of oligemia produced by partial occlusion of the middle cerebral artery. Magn Reson Med 2000;44:706–12.
95. Zaharchuk G, Yamada M, Sasamata M, Jenkins BG, Moskowitz MA, Rosen BR. Is all perfusion-weighted magnetic resonance imaging for stroke equal? The temporal evolution of multiple hemodynamic parameters after focal ischemia in rats correlated with evidence of infarction. J Cereb Blood Flow Metab 2000;20:1341–51.
96. Pillekamp F, Grune M, Brinker G, Franke C, Uhlenkuken U, Hoehn M, et al. Magnetic resonance prediction of outcome after thrombolytic treatment. Magn Reson Imaging 2001;19:143–52.
97. Chalela JA, Alsop DC, Gonzalez-Atavales JB, Maldjian JA, Kasner SE, Detre JA. Magnetic resonance perfusion imaging in acute ischemic stroke using continuous arterial spin labeling. Stroke 2000;31:680–7.
98. Siewert B, Schlaug G, Edelman RR, Warach S. Comparison of EPISTAR and T2*-weighted gadolinium-enhanced perfusion imaging in patients with acute cerebral ischemia. Neurology 1997;48:673–9.

99. Davies NP, Jezzard P. Selective arterial spin labeling (SASL): perfusion territory mapping of selected feeding arteries tagged using two-dimensional radiofrequency pulses. Magn Reson Med 2003;49:1133–42.
100. Hendrikse J, van der Grond J, Lu H, van Zijl PC, Golay X. Flow territory mapping of the cerebral arteries with regional perfusion MRI. Stroke 2004;35:882–7.
101. Trampel R, Mildner T, Goerke U, Schaefer A, Driesel W, Norris DG. Continuous arterial spin labeling using a local magnetic field gradient coil. Magn Reson Med 2002;48:543–6.
102. Werner R, Norris DG, Alfke K, Mehdorn HM, Jansen O. Continuous artery-selective spin labeling (CASSL). Magn Reson Med 2005;53:1006–12.
103. van Laar PJ, Hendrikse J, Golay X, Lu H, van Osch MJ, van der GJ. In-vivo flow territory mapping of major brain feeding arteries. Neuroimage 2006;29:136–44.
104. Brown SL, Ewing JR, Kolozsvary A, Butt S, Cao Y, Kim JH. Magnetic resonance imaging of perfusion in rat cerebral 9L tumor after nicotinamide administration. Int J Radiat Oncol Biol Phys 1999;43:627–33.
105. Gaa J, Warach S, Wen P, Thangaraj V, Wielopolski P, Edelman RR. Noninvasive perfusion imaging of human brain tumors with EPISTAR. Eur Radiol 1996;6:518–22.
106. Silva AC, Kim SG, Garwood M. Imaging blood flow in brain tumors using arterial spin labeling. Magn Reson Med 2000;44:169–73.
107. Warmuth C, Gunther M, Zimmer C. Quantification of blood flow in brain tumors: comparison of arterial spin labeling and dynamic susceptibility-weighted contrast-enhanced MR imaging. Radiology 2003;228:523–32.
108. Altes TA, Mai VM, Munger TM, Brookeman JR, Hagspiel KD. Pulmonary embolism: comprehensive evaluation with MR ventilation and perfusion scanning with hyperpolarized helium-3, arterial spin tagging, and contrast-enhanced MRA. J Vasc Interv Radiol 2005;16:999–1005.
109. Lipson DA, Roberts DA, Hansen-Flaschen J, Gentile TR, Jones G, Thompson A, et al. Pulmonary ventilation and perfusion scanning using hyperpolarized helium-3 MRI and arterial spin tagging in healthy normal subjects and in pulmonary embolism and orthotopic lung transplant patients. Magn Reson Med 2002;47:1073–6.
110. Mai VM, Hagspiel KD, Altes T, Goode AR, Williams MB, Berr SS. Detection of regional pulmonary perfusion deficit of the occluded lung using arterial spin labeling in magnetic resonance imaging. J Magn Reson Imaging 2000;11:97–102.
111. Uematsu H, Levin DL, Hatabu H. Quantification of pulmonary perfusion with MR imaging: recent advances. Eur J Radiol 2001;37:155–63.
112. Belle V, Kahler E, Waller C, Rommel E, Voll S, Hiller KH, et al. In vivo quantitative mapping of cardiac perfusion in rats using a noninvasive MR spin-labeling method. J Magn Reson Imaging 1998;8:1240–5.
113. Floyd TF, McGarvey M, Ochroch EA, Cheung AT, Augoustides JA, Bavaria JE, et al. Perioperative changes in cerebral blood flow after cardiac surgery: influence of anemia and aging. Ann Thorac Surg 2003;76:2037–42.
114. Reeder SB, Atalay MK, McVeigh ER, Zerhouni EA, Forder JR. Quantitative cardiac perfusion: a noninvasive spin-labeling method that exploits coronary vessel geometry. Radiology 1996;200:177–84.
115. Berr SS, Hagspiel KD, Mai VM, Keilholz-George S, Knight-Scott J, Christopher JM, et al. Perfusion of the kidney using extraslice spin tagging (EST) magnetic resonance imaging. J Magn Reson Imaging 1999;10:886–91.
116. De Bazelaire C, Rofsky NM, Duhamel G, Michaelson MD, George D, Alsop DC. Arterial spin labeling blood flow magnetic resonance imaging for the characterization of metastatic renal cell carcinoma(1). Acad Radiol 2005;12: 347–57.
117. Karger N, Biederer J, Lusse S, Grimm J, Steffens J, Heller M, et al. Quantitation of renal perfusion using arterial spin labeling with FAIR-UFLARE. Magn Reson Imaging 2000;18:641–7.
118. Prasad PV, Kim D, Kaiser AM, Chavez D, Gladstone S, Li W, et al. Noninvasive comprehensive characterization of renal artery stenosis by combination of STAR angiography and EPISTAR perfusion imaging. Magn Reson Med 1997;38:776–87.
119. Wang JJ, Hendrich KS, Jackson EK, Ildstad ST, Williams DS, Ho C. Perfusion quantitation in transplanted rat kidney by MRI with arterial spin labeling. Kidney Int 1998;53:1783–91.
120. Detre JA, Zhang W, Roberts DA, Silva AC, Williams DS, Grandis DJ, et al. Tissue specific perfusion imaging using arterial spin labeling. NMR Biomed 1994;7:75–82.
121. Wong EC, Buxton RB, Frank LR. Implementation of quantitative perfusion imaging techniques for functional brain mapping using pulsed arterial spin labeling. NMR Biomed 1997;10:237–49.
122. Jahng GH, Zhu XP, Matson GB, Weiner MW, Schuff N. Improved perfusion-weighted MRI by a novel double inversion with proximal labeling of both tagged and control acquisitions. Magn Reson Med 2003;49:307–14.
123. Chen Q, Siewert B, Bly BM, Warach S, Edelman RR. STAR–HASTE: perfusion imaging without magnetic susceptibility artifact. Magn Reson Med 1997;38:404–8.
124. Petersen ET, Lim TC, Golay X. A model-free arterial spin labeling quantitative approach for perfusion MRI. Magn Reson Med 2006;55:219–32.
125. Schwarzbauer C, Morrissey SP, Haase A. Quantitative magnetic resonance imaging of perfusion using magnetic labeling of water proton spins within the detection slice. Magn Reson Med 1996;35:540–6.
126. Tanabe JL, Yongbi M, Branch C, Hrabe J, Johnson G, Helpern JA. MR perfusion imaging in human brain using the UNFAIR technique. Un-inverted flow-sensitive alternating inversion recovery. J Magn Reson Imaging 1999;9:761–7.
127. Mai VM, Berr SS. MR perfusion imaging of pulmonary parenchyma using pulsed arterial spin labeling techniques: FAIRER and FAIR. J Magn Reson Imaging 1999;9:483–7.
128. Mai VM, Hagspiel KD, Christopher JM, Do HM, Altes T, Knight-Scott J, et al. Perfusion imaging of the human lung using flow-sensitive alternating inversion recovery with an extra radiofrequency pulse (FAIRER). Magn Reson Imaging 1999;17:355–61.
129. Zhou J, van Zijl PC. Perfusion imaging using FAIR with a short predelay. Magn Reson Med 1999;41:1099–107.
130. Zhou J, Mori S, van Zijl PC. FAIR excluding radiation damping (FAIRER). Magn Reson Med 1998;40:712–9.
131. Schwarzbauer C, Heinke W. BASE imaging: a new spin labeling technique for measuring absolute perfusion changes. Magn Reson Med 1998;39:717–22.